ARTICLE OPEN

Check for updates

Impact of *KRAS* mutations and co-mutations on clinical outcomes in pancreatic ductal adenocarcinoma

Abdelrahman Yousef[1], Mahmoud Yousef[1], Saikat Chowdhury[1], Kawther Abdilleh[2], Mark Knafl[3], Paul Edelkamp[4], Kristin Alfaro-Munoz[1], Ray Chacko[1], Jennifer Peterson[1], Brandon G. Smaglo[1], Robert A. Wolff[1], Shubham Pant[1], Michael S. Lee[1], Jason Willis[1], Michael Overman[1], Sudheer Doss[2], Lynn Matrisian[2], Mark W. Hurd[5], Rebecca Snyder[6], Matthew H. G. Katz[6], Huamin Wang[7], Anirban Maitra[5,7], John Paul Shen[1] and Dan Zhao[1]✉

The relevance of *KRAS* mutation alleles to clinical outcome remains inconclusive in pancreatic adenocarcinoma (PDAC). We conducted a retrospective study of 803 patients with PDAC (42% with metastatic disease) at MD Anderson Cancer Center. Overall survival (OS) analysis demonstrated that *KRAS* mutation status and subtypes were prognostic ($p < 0.001$). Relative to patients with *KRAS* wildtype tumors (median OS 38 months), patients with $KRAS^{G12R}$ had a similar OS (median 34 months), while patients with $KRAS^{Q61}$ and $KRAS^{G12D}$ mutated tumors had shorter OS (median 20 months [HR: 1.9, 95% CI 1.2–3.0, $p = 0.006$] and 22 months [HR: 1.7, 95% CI 1.3–2.3, $p < 0.001$], respectively). There was enrichment of $KRAS^{G12D}$ mutation in metastatic tumors (34% vs 24%, OR: 1.7, 95% CI 1.2–2.4, $p = 0.001$) and enrichment of $KRAS^{G12R}$ in well and moderately differentiated tumors (14% vs 9%, OR: 1.7, 95% CI 1.05–2.99, $p = 0.04$). Similar findings were observed in the external validation cohort (PanCAN's Know Your Tumor® dataset, $n = 408$).

npj Precision Oncology (2024)8:27 ; https://doi.org/10.1038/s41698-024-00505-0

INTRODUCTION

Pancreatic ductal adenocarcinoma (PDAC) is projected to be the second leading cause of cancer death in the US by 2040; with limited available treatment options for metastatic PDAC, the 5-year survival rate is <5%[1,2]. The median overall survival (OS) for the current standard of care chemotherapy (oxaliplatin, irinotecan, fluorouracil, and leucovorin [FOLFIRINOX]) is 11.1 months in the first-line treatment of metastatic disease, with an objective response rate (ORR) of 31.6% and median progression-free survival (PFS) of 6.4 months[3,4]. The median OS for the other available first-line chemotherapy regimen, gemcitabine/nab-paclitaxel, is 8.5 months with an ORR of 23% and median PFS of 5.5 months[5]. In the setting of second-line treatment, the median OS with chemotherapy (liposomal irinotecan, fluorouracil and leucovorin) is only 6.1 months, with an ORR of 16% and median PFS of 3.1 months[6]. Better therapy for PDAC is urgently needed.

Among the identified genomic alterations (GAs) in PDAC, oncogenic *KRAS* mutations are the most common, occurring in close to 90% of patients, followed by *TP53*, *CDKN2A*, and *SMAD4*[7,8]. The majority of *KRAS* mutations are at codon 12, with the highest prevalence of G12D mutation (35%), followed by G12V (20–30%), G12R (10–20%), Q61 (~5%), G12C (1–2%), and other rare muations[9–12]. Targeting *KRAS* has been challenging for decades until allosteric $KRAS^{G12C}$ mutant-specific inhibition by covalent binding to the mutant cysteine beneath the switch-II region, which locks it in the inactive GDP bound form was discovered[13]. Exciting results from clinical trials of the $KRAS^{G12C}$ inhibitors sotorasib (AMG510) and adagrasib (MRTX849) have been reported, and both have been approved by the US FDA for previously treated $KRAS^{G12C}$-mutated advanced lung cancer. Moreover, efficacy of both sotorasib and adagrasib against PDAC has also been observed[14–18]. Sotorasib had a 21% ORR with a median PFS of 4.0 months in patients with pancreatic cancer who had received chemotherapy previously[19]. Adagrasib monotherapy had an ORR of 33.3% with a median PFS of 5.4 months (95% CI 3.9–8.2) and a median OS of 8.0 months (95% CI 5.2–11.8) in patients with pancreatic cancer refractory to chemotherapy ($n = 21$)[20]. Furthermore, preclinical development of a $KRAS^{G12D}$ inhibitor (MRTX 1133) has shown promising results and MRTX 1133 is currently in phase 1 clinical trial[21]. Most recently, pan-*KRAS* inhibitor RMC-6236, which binds to the chaperone protein cyclophilin A and active GTP-bound RAS (RAS ON inhibitor), is also being tested in patients (NCT05379985). Finally, T cell therapy with $KRAS^{G12D}$-targeting T cell receptors (TCRs) caused tumor regression in a patient with pancreatic cancer, and T cells with TCRs targeting other *KRAS* mutations, such $KRAS^{G12V}$, are under development[22,23].

We are at a breakthrough point in attempts to target *KRAS* in pancreatic cancer. The remaining challenges include the short duration of response and primary/secondary resistance to *KRAS* inhibition. Additionally, while multiple genomic and non-genomic factors have been associated with resistance to *KRAS* inhibitors, such as co-mutations of *KEAP1/STK11* with *KRAS* as observed in patients with lung cancer, *KEAP1/STK11* co-mutations are rare in pancreatic cancer, and little is known about the landscape of *KRAS* mutations and co-mutations in pancreatic cancer or their impact on clinical outcomes[12,24,25].

KRAS-mutated cancers are heterogeneous with different mutation allele subtypes and co-mutations[26–28]. Each *KRAS* mutation allele subtype has unique biochemical and clinicopathological features, and the differences between the mutation subtypes and

[1]Department of Gastrointestinal Medical Oncology, The University of Texas MD Anderson Cancer Center, Houston, TX, USA. [2]Pancreatic Cancer Action Network, Manhattan Beach, Los Angeles, CA, USA. [3]Department of Genomic Medicine, The University of Texas MD Anderson Cancer Center, Houston, TX, USA. [4]Department of Data Engineering & Analytics, The University of Texas MD Anderson Cancer Center, Houston, TX, USA. [5]Sheikh Ahmed Center for Pancreatic Cancer Research, The University of Texas MD Anderson Cancer Center, Houston, TX, USA. [6]Department of Surgical Oncology, The University of Texas MD Anderson Cancer Center, Houston, TX, USA. [7]Department of Translational Molecular Pathology, The University of Texas MD Anderson Cancer Center, Houston, TX, USA. ✉email: dzhao3@mdanderson.org

co-mutations in pancreatic cancer have not been well studied[26–29]. The *KRAS*^{G12D} mutation has an intrinsic wildtype and SOS1 guanine exchange activities while the *KRAS*^{Q61} mutation has deficiencies in GTP hydrolysis[27,30]. The *KRAS*^{G12R} mutation, which accounts for approximately 15% of the *KRAS* mutations in pancreatic cancer but less than 1% of the *KRAS* mutations in lung cancer, was reported to be associated with different downstream signaling pathways relative to other *KRAS* mutations[27]. The *KRAS*^{G12D} mutation was reported to be more immune suppressive with shorter survival in lung cancer and pancreatic cancer[31,32]. Moreover, it has been reported that genes most frequently co-mutated with *KRAS* vary with the *KRAS* mutation alleles in patients with lung cancer, and these different patterns of co-mutation with *KRAS* differentially affect clinical outcomes[33]. For example, co-mutation of *KEAP1/STK11* was more common in patients with *KRAS*^{G13}-mutated lung cancer than in patients with *KRAS*^{G12D}-mutated lung cancer, and co-mutation of *KEAP1/STK11* with *KRAS*^{G13} was associated with poor prognosis and treatment resistance[28].

Research to date on the impact of *KRAS* allele subtypes and co-mutations on PDAC clinical outcomes has been limited, and the conclusions remain controversial. Compared to *KRAS*^{G12R}-mutated PDAC, *KRAS*^{G12D}-mutated PDAC was reported to be associated with worse OS in a single institutional study ($n = 126$); however, within the *KRAS*^{G12R}-mutated PDAC group, those with *PI3K* pathway co-mutations experienced worse OS[34]. Meanwhile, another study found no statistically significant difference in OS between different *KRAS* mutation alleles[12]. Our institution has collaborated with the data science firm Syntropy to deploy the Palantir Foundry software platform for extraction and analysis of merged clinical and laboratory data across a variety of platforms, including the Electronic Health Record (EHR), molecular testing/next generation sequencing (NGS), pathology and radiology results, and tumor registry data[35–37]. Together with the development of data science tools such as natural language processing (NLP) and the increased use of NGS in pancreatic cancer, the Foundry platform now gives us the ability to analyze large datasets comprising real-world clinical and molecular information to dissect the heterogeneity of *KRAS*-mutated pancreatic cancer. In this study, we illustrate the co-mutation landscape of *KRAS* mutations and the allele-specific associations of *KRAS*-mutated pancreatic cancer with clinical outcome in our institution. In addition, we validated our findings in an external cohort from the Pancreatic Cancer Action Network (PanCAN)'s Know Your Tumor® (KYT) Dataset[38].

RESULTS

Patient characteristics

A total of 803 patients with PDAC who had tumor tissue somatic mutation testing performed at MD Anderson were identified (Fig. 1); the demographic and clinical characteristics of this cohort are summarized in Table 1. The median age was 63 years (range 26–86), 43% were female, and 29.3% had a smoking history (current or former). A total of 336 (42%) patients had documented stage IV disease at the time of their initial diagnosis, and 321 (40%) had poorly differentiated tumors. *KRAS* gene mutation status was tested in 703 patients, including 302 with stage IV disease; 578 (82%) were positive for mutated *KRAS*. In addition to *KRAS, TP53* was tested in 604 patients, 418 (69%) of whom were positive; *CDKN2A* was tested in 509 patients, 102 (20%) of whom were positive; and *SMAD4* was tested in 536 patients, 68 (13%) of whom were positive. The median follow-up time from the initial diagnosis was 41 months. Median OS of the entire cohort of 803 patients was 19 months (range 0.07–348).

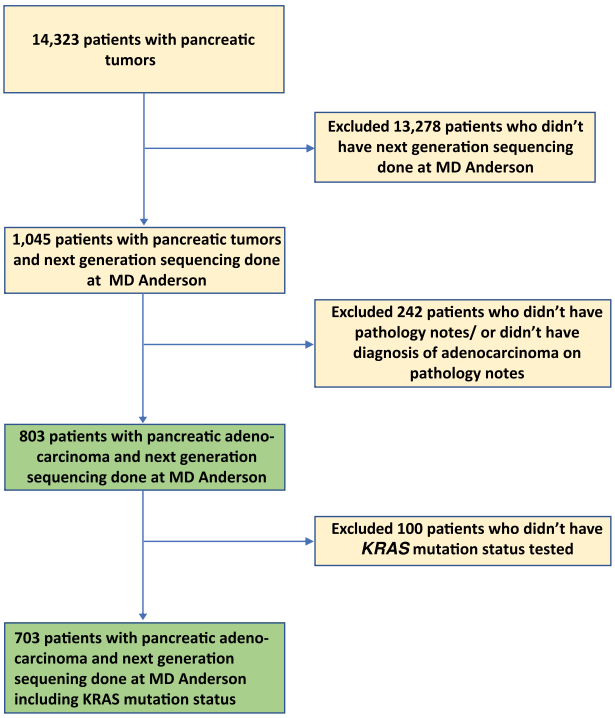

Fig. 1 Study flowchart diagram. The flowchart shows cohort patient selection. Abbreviations include MD Anderson (MD Anderson Cancer Center).

KRAS mutation status and allele subtype association with OS

Among the 578 patients whose tumors tested positive for a *KRAS* mutation, 227 had *KRAS*^{G12D} (39%), 182 had *KRAS*^{G12V} (31%), 81 had *KRAS*^{G12R} (14%), 35 had *KRAS*^{Q61} (6%), and 53 had other uncommon *KRAS* variants (9%) (Fig. 2d). The Kaplan–Meier (KM) analysis of OS in all 703 patients with known *KRAS* mutation status (all stages included) demonstrated that *KRAS* mutation status and subtype was prognostic of OS ($p < 0.001$) (Fig. 2a); patients with *KRAS* wildtype tumors had a median OS of 38 months, patients with *KRAS*^{G12R} tumors had a median OS of 34 months (HR: 1, 95% CI 0.71–1.5, $p = 0.88$), patients with *KRAS*^{Q61} tumors had a median OS of 20 months (HR: 1.9, 95% CI 1.2–3.0, $p = 0.006$), and patients with *KRAS*^{G12D} tumors had a median OS of 22 months (HR: 1.7, 95% CI 1.3–2.3, $p < 0.001$) (Fig. 2c). When limited to patients with stage IV metastatic disease ($n = 302$), *KRAS* mutation remained significantly associated with OS ($p = 0.034$) (Fig. 2b). Again, patients with *KRAS*^{Q61} and *KRAS*^{G12D} mutations had shorter median OS (15 and 11 months, respectively) relative to those with *KRAS*^{G12R}-mutated and *KRAS* wildtype tumors (median OS of 25 and 24 months respectively). *KRAS*^{G12D}-mutated tumors (HR = 1.7, 95% CI 1.1–2.6, $p = 0.009$) were associated with significantly worse OS relative to *KRAS* wildtype tumors.

KRAS mutation allele subtype association with stage and tumor differentiation

Advanced disease stage was associated with decreased OS ($p < 0.001$). Patients with stage IV PDAC had median OS of 16 months (HR: 3.3, 95% CI 2.4–4.4) while patients with stage I PDAC had a median OS of 48 months (Fig. 3a). In the full cohort of patients with known *KRAS* mutation status (all stages included), tumor histopathology was also prognostic of OS ($p < 0.001$); poorly differentiated/anaplastic tumors had shorter overall survival (median OS = 21 months; HR: 2.3, 95% CI 1.4-3.9) than patients with well-differentiated tumors (median OS = 62 months) (Fig. 3b). We also found a greater prevalence of *KRAS*^{G12D} mutations in patients with metastatic disease (stage IV) than in patients with

Table 1. MDA cohort patient characteristics.

All	803 (100%)
Age, years–median (range)	63 (26, 86)
Race/ethnicity	
Asian	56 (7.0%)
Black or African	55 (6.8%)
Hispanic or Latino	74 (9.2%)
White or Caucasian	587 (73.1%)
Other	31 (3.9%)
Sex	
Female	345 (43.0%)
Male	458 (57.0%)
Smoking status	
Current smoker	36 (4.5%)
Former smoker	199 (24.8%)
Never	372 (46.3%)
Not available	196 (24.4%)
Histology grade	
Well-differentiated	29 (3.6%)
Moderately differentiated	300 (37.4%)
Poorly differentiated	321 (40.0%)
Undifferentiated	4 (0.5%)
Not available	149 (18.6%)
Stage at diagnosis	
I	122 (15.2%)
II	138 (17.2%)
III	105 (13.1%)
IV	336 (41.8%)
Not available	102 (12.7%)
KRAS ($n = 703$)	
Mutant	578 (82%)
Wildtype	125 (18%)
TP53 ($n = 604$)	
Mutant	418 (69%)
Wildtype	186 (31%)
CDKN2A ($n = 509$)	
Mutant	102 (20%)
Wildtype	407 (80%)
SMAD4 ($n = 536$)	
Mutant	68 (13%)
Wildtype	468 (87%)
OS, months—median (range)	19 (0.07, 348)

localized disease (stage I–III) (34% vs. 24%, OR:1.7, 95% CI:1.2–2.4, $p = 0.001$) (Fig. 3c) and an increased prevalence of *KRAS*^{G12R} mutations in well and moderately differentiated tumors than in poorly differentiated/anaplastic tumors (14% vs. 9%, OR:1.7, 95% CI: 1.05–2.99, $p = 0.04$) (Fig. 3d).

KRAS Co-mutations and OS

The top detected GAs (Fig. 4a) were sorted by the detected positivity rate among tested patients (the number of tested patients for each gene varied due to different gene panels in the testing platforms). *KRAS* (82%, $N = 578$ of 703), *TP53* (69%, $N = 418$ of 608), *CDKN2A* (20%, $N = 102$ of 509), *SMAD4* (13%, $N = 68$ of 536), and *ARID1A* (7%, $N = 34$ of 482) were the most commonly mutated genes in the MD Anderson cohort (Fig. 4c). *TP53* was the most frequently detected co-mutation with *KRAS*, with a 67% *TP53* co-positive rate, followed by *CDKN2A* (17%), *SMAD4* (11%), and *ARID1A* (6%) (Fig. 4b). In the co-mutation analysis, *KRAS* was found to be frequently co-mutated with *TP53* (OR: 1.77, 95% CI 0.85–3.6, false discovery rate (FDR)-corrected $p = 0.29$), and *CDKN2A* (OR: 2.05, 95% CI 0.71–8.13, FDR-corrected $p = 0.47$). Interestingly, *KRAS* and *GNAS* were mutually exclusive (OR: 0.23, 95% CI 0.07–1.05, FDR-corrected $p = 0.14$) while *TP53* and *ATM* were mutually exclusive (OR: 0.31, 95% CI 0.12–0.81, FDR-corrected $p = 0.095$). (Fig. 5a). Moreover, *TP53* and *CDKN2A* were frequently co-mutated (OR: 2.11, 95% CI 1.17–4.04, FDR-corrected $p = 0.095$). Also, *ARID1A* was found to be significantly co-mutated with *CDKN2A* (OR: 2.7, 95% CI 1.18–6.02, FDR-corrected $p = 0.095$) and *SMARCA4* (OR: 5.17, 95% CI 1.15–8.44, FDR-corrected $p = 0.1$).

In univariate Cox proportional hazards analysis for the most commonly mutated genes in the MD Anderson cohort, *ARID1A* mutation was associated with poor OS, with median OS of 18 months in patients with *ARID1A*-mutated tumors vs 31 months in patients with *ARID1A* wildtype tumors (HR: 1.6, 95% CI 0.99–2.6, $p = 0.05$). However, *SMAD4* mutant tumors had better OS than *SMAD4* wildtype tumors (median OS 35 and 27 months, respectively, HR: 0.67, 95% CI 0.46–0.99, $p = 0.046$) (Fig. 5b). Interestingly, while none of the patients with *KRAS*^{G12R}-mutated tumors had *ARID1A* co-mutation, *ARID1A* co-mutation was observed in 8% of *KRAS*^{G12D} mutated tumors ($p = 0.02$). Conversely, *SMAD4* co-mutation was observed in 15% of the patients with *KRAS*^{G12R}-mutated tumors compared with 10% in patients with *KRAS*^{G12D}-mutated tumors ($p = 0.22$) (Fig. 4b).

In patients with metastatic disease and known *KRAS*, *TP53*, and *CDKN2A* mutation status ($n = 232$), we classified four distinct molecular subtypes of metastatic PDAC (Fig. 5c): (1) *KRAS* mutant predominant (*KRAS* mutant, *TP53* wildtype/*CDKN2A* wildtype) ($n = 46/232$), (2) *TP53* mutant predominant (*TP53* mutant, *KRAS* mutant or wildtype/*CDKN2A* wildtype) ($n = 127/232$), (3) *CDKN2A* mutant predominant (*CDKN2A* mutant, *KRAS* mutant or wildtype/*TP53* mutant or wildtype) ($n = 41/232$), and (4) triple negative (all *KRAS, TP53*, and *CDKN2A* wildtype) ($n = 18/232$). Patients with triple negative (*KRAS-/TP53-/CDKN2A-)* tumors had the longest median OS (28 months), while the *CDKN2A* predominant group had the worst OS (median 12 months); the *TP53* predominant group (median 17 months) and *KRAS* predominant group (median 14 months) had intermediate OS ($p = 0.014$) (Fig. 5c). PanCAN's Know Your Tumor® (KYT) Dataset.

To validate our findings, an external cohort from PanCAN's KYT dataset ($n = 408$) was analyzed. Baseline characteristics of patients in the KYT cohort are summarized in Table 2. The median age at the time of diagnosis was 65 years (range 36–88); 46% were female and 54% were male. The median follow-up time from diagnosis was 15 months. While disease staging information was not available for the majority of the patients in this cohort (59.8%); among those with known stage, 23.8% ($n = 97$) had documented stage IV disease at the time of diagnosis. Median overall survival in all the patients was 22 months (range 0.2–93 months). *KRAS* (92%), *TP53* (77%), *SMAD4* (24%), *CDKN2A* (21%), and *ARID1A* (5%) were the most commonly mutated genes in the PanCAN cohort (Fig. 6a).

Similar to the MD Anderson cohort, *TP53* was the most frequently detected co-mutation with *KRAS*, (73% positive rate), followed by *CDKN2A* (20%), *SMAD4* (22%), and *ARID1A* (5%) (Fig. 6b). In the co-mutation analysis (Fig. 7a), *KRAS* was found to be frequently co-mutated with *TP53* (OR: 2.6, FDR-corrected $p = 0.18$), and *CDKN2A* (OR: 2.6, FDR-corrected $p = 0.84$). *TP53* and *CDKN2A* were frequently co-mutated (OR: 3.54, FDR-corrected $p = 0.009$). *TP53* mutation was mutually exclusive with both *ATM* (OR: 0.04, FDR-corrected $p = 9.8E-07$) and *GNAS* (OR: 0.05, FDR-corrected $p = 6.65E-05$) mutations. *KRAS* and *GNAS* mutations were also mutually exclusive (OR: 0.17, FDR-corrected $p = 0.18$) (Fig. 7a). *KRAS*^{G12R} was associated with significantly longer median

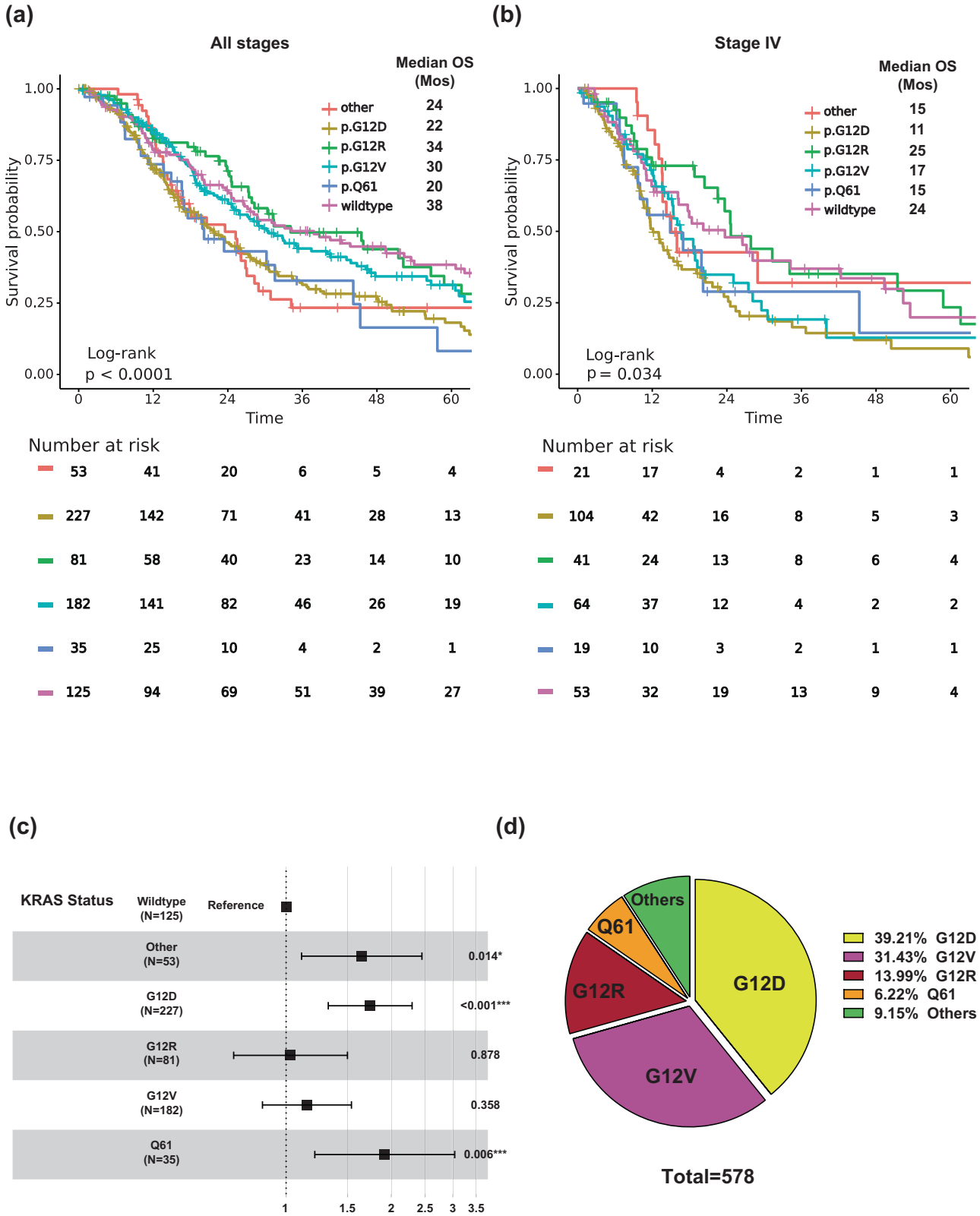

Fig. 2 Overall survival (OS) with *KRAS* mutations and mutation subtypes. a KM OS curves of all patients, and stage IV patients only **b** with *KRAS*-mutated PDAC **c** Univariate analysis of OS with *KRAS* mutation subtypes and **d** Frequencies of different *KRAS* mutations in patients with *KRAS*-mutant PDAC ($n = 578$).

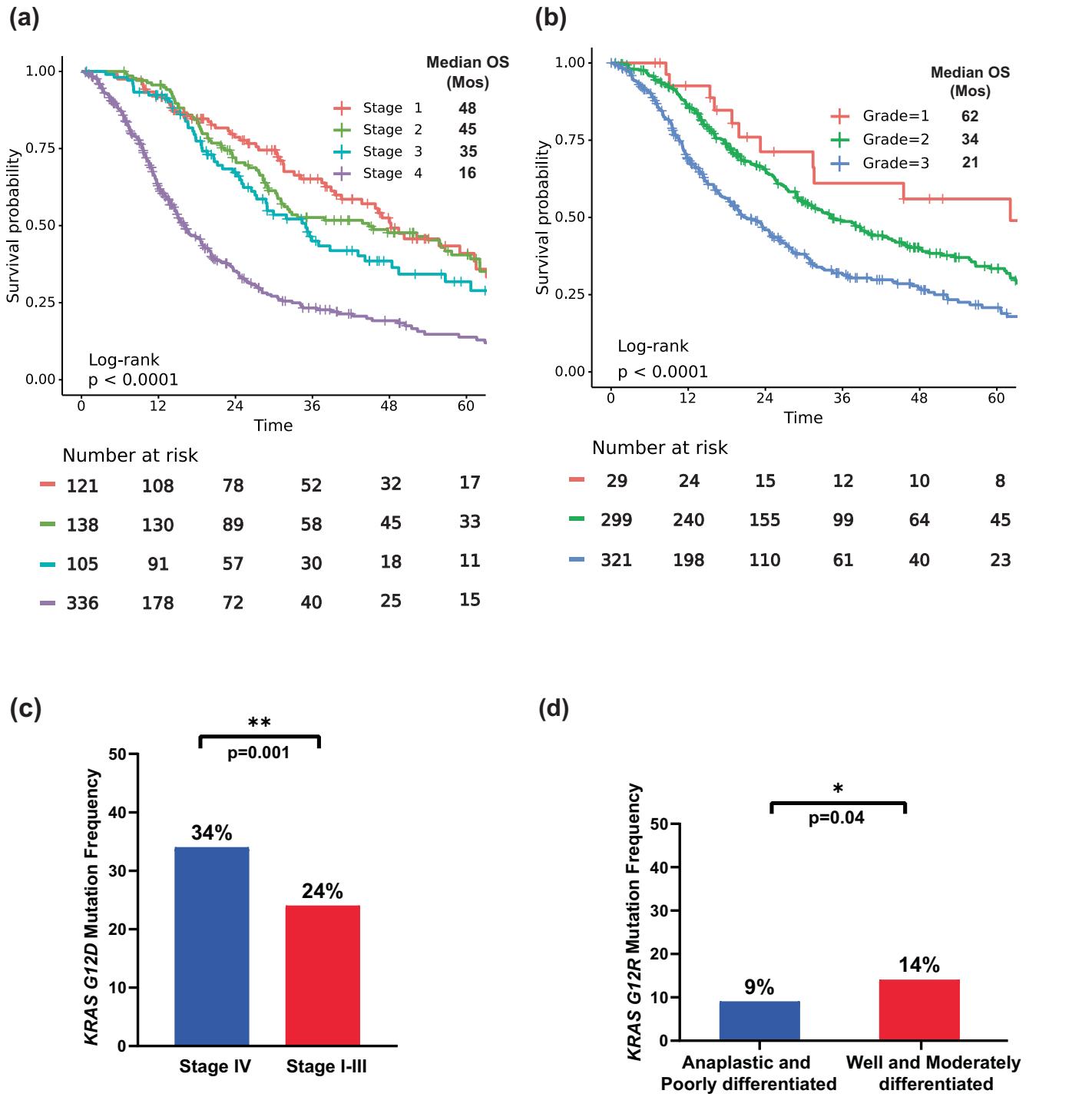

Fig. 3 OS with stage and histopathological grade and KRAS mutations. a KM OS curves for tumor stage of our cohort. **b** KM OS curves for tumor histopathological grade of our cohort. **c** Bar plot showing enrichment of $KRAS^{G12D}$ mutation in metastatic disease. **d** Bar plot showing enrichment of $KRAS^{G12R}$ in well and moderately differentiated tumors.

OS (32 months) than $KRAS^{Q61}$ (16 months, HR: 2.6, 95% CI 0.88–7.8, $p = 0.02$) and $KRAS^{G12D}$ (23 months, HR: 1.68, 95% CI 1.06–2.65, $p = 0.04$) (Fig. 7b).

DISCUSSION

In this study, we analyzed the impact of *KRAS* mutation status, *KRAS* allele subtypes, and co-occurring mutations on clinical outcome of patients with PDAC in two real-world datasets. The study included 803 patients who had been tested for somatic tumor mutations at MD Anderson Cancer Center and an external cohort ($n = 408$) of patients with pancreatic cancer from the PanCAN KYT® dataset. We found that *KRAS* mutation status and allele subtypes were associated with OS; median OS was longer in patients with *KRAS* wildtype and $KRAS^{G12R}$-mutated tumors compared to median OS in patients with $KRAS^{G12D}$ or $KRAS^{Q61}$-mutated tumors. We illustrated the co-mutation landscape with *KRAS* mutation. We also found that *ARID1A* mutation was

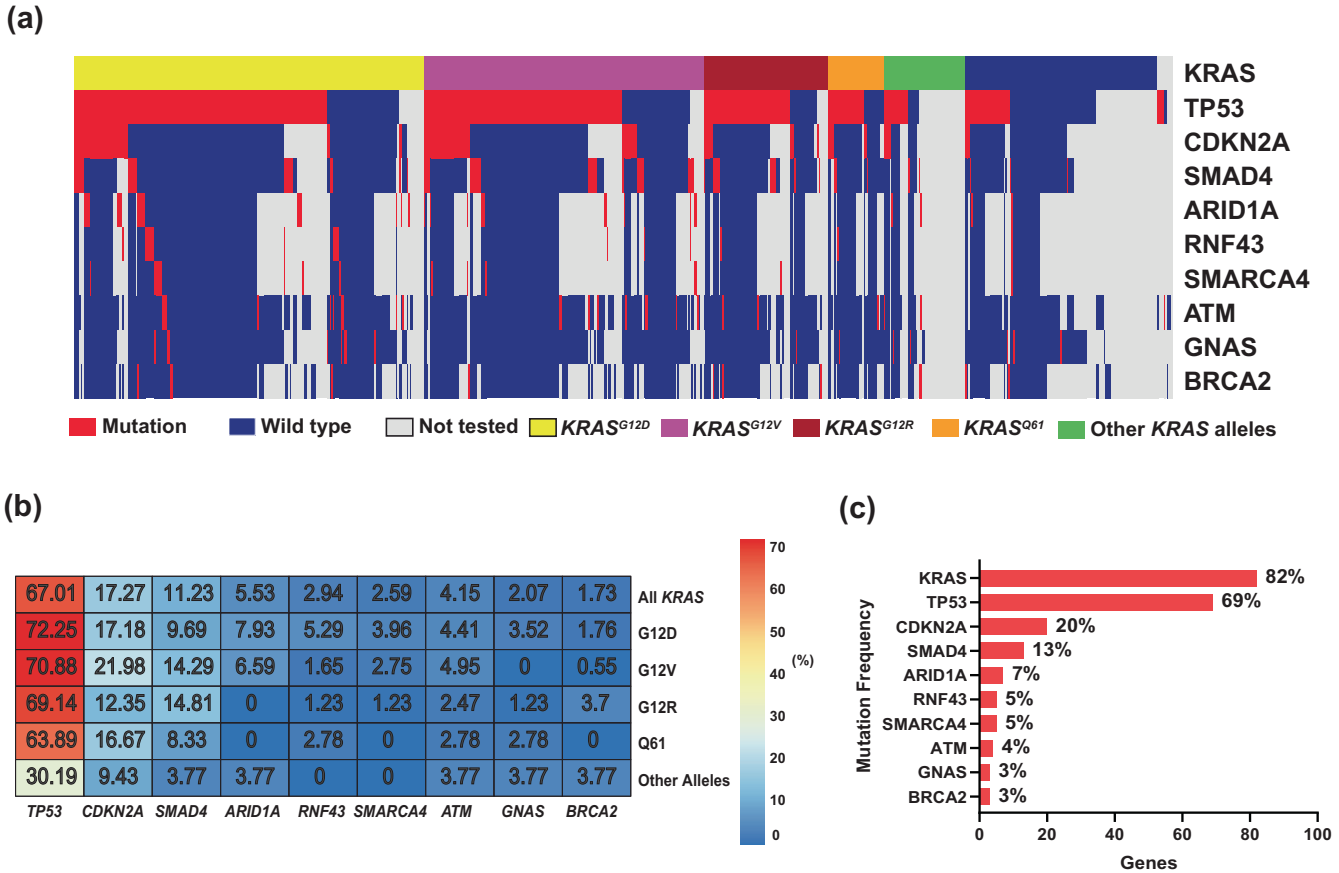

Fig. 4 Allele-specific co-mutations with KRAS in the MDA cohort. a Oncoplot showing the distribution of different *KRAS* mutational subtypes with the different genes in our cohort. **b** Heatmap showing the co-mutation landscape of the different *KRAS* mutation subtypes with the different genes and their frequencies. **c** Bar plot showing the most frequently mutated genes in our cohort.

associated with worse OS and *SMAD4* was associated with better OS. We found *TP53* and *ATM* mutations were mutually exclusive. There was a higher rate of *ARID1A* mutation in $KRAS^{G12D}$ compared with $KRAS^{G12R}$ patients. We also found enrichment of $KRAS^{G12D}$ in metastatic disease and enrichment of $KRAS^{G12R}$ in well to moderately differentiated tumors.

Among the 803 patients with PDAC tested for somatic tumor mutations at MD Anderson, 703 were tested for *KRAS* mutations (Fig. 1). The overall positive rate for *KRAS* mutation was 82% ($n = 578$); the most common mutation was $KRAS^{G12D}$ (39%), followed by $KRAS^{G12V}$ (31%), $KRAS^{G12R}$ (14%), $KRAS^{Q61}$ (6%), and other uncommon *KRAS* variants (9%) (Fig. 2d). There were differences in OS with *KRAS* mutation status and allele subtypes in both the overall population (all stages, Fig. 2a) and in the subset of patients with stage IV disease ($n = 302$) (Fig. 2b). Compared to patients with *KRAS* wildtype tumors, regardless of disease stages, patients with $KRAS^{G12D}$ (median OS 22 months, HR: 1.7, 95% CI 1.3–2.3, $p < 0.001$) or $KRAS^{Q61}$ (median OS 20 months, HR: 1.9, 95% CI 1.2–3.0, $p = 0.006$) mutated tumors had worse survival. $KRAS^{G12R}$ mutated patients (median OS 34 months, HR: 1, 95% CI 0.71–1.5, $p = 0.88$) had similar OS as wildtype patients (median OS 38 months, reference) (Fig. 2c). The external cohort from the PanCAN KYT® dataset ($n = 408$) validated the finding that $KRAS^{G12R}$ mutation was associated with the longest median OS (32 months), while $KRAS^{Q61}$ (16 months, HR: 2.6, 95% CI 0.88–7.8, $p = 0.02$) and $KRAS^{G12D}$ mutations (23 months, HR: 1.68, 95% CI 1.06–2.65, $p = 0.04$) were associated with shorter median OS (Fig. 7b). Our results were consistent with the previous report of significantly longer OS (HR 0.55) in patients with $KRAS^{G12R}$-mutated PDAC ($n = 23$) compared with those with non-$KRAS^{G12R}$ PDAC ($n = 88$)[34]. Another study comparing $KRAS^{G12C}$ ($n = 30$) and other *KRAS* mutations reported longer median OS (starting from the first line therapy, $p = 0.03$) for *KRAS* wildtype tumors ($n = 91$) in patients with metastatic PDAC, which was consistent with our findings of better survival in *KRAS* wildtype patients[12]; however, the authors did not show statistically significant difference between other *KRAS* alleles while compared against $KRAS^{G12C}$ patients[12]. Due to the low frequency of $KRAS^{G12C}$ mutation, we grouped the patients with $KRAS^{G12C}$ mutations with patients that had other uncommon mutations. In our cohort, OS was defined from initial diagnosis and there was enrichment of $KRAS^{G12D}$ mutation in metastatic disease (stage IV) (OR: 1.7, 95% CI 1.2–2.4, $p = 0.001$) (Fig. 3c). Our data suggested worse outcomes in patients with $KRAS^{G12D}$ tumors. This is consistent with a previous study of 356 patients with resected PDAC, which reported that those with *KRAS* mutations had worse disease-free survival (DFS) (median 12.3 months) and OS (median 20.3 months) compared with those with wildtype *KRAS* (DFS 16.2 months and OS 38.6 months), and particularly poor outcomes were observed in patients with $KRAS^{G12D}$ mutation (median OS 15.3 months)[39].

The mechanisms of why $KRAS^{G12D}$ is associated with poor prognosis relative to the other subtypes is not fully understood beyond the co-mutation with *ARID1A* and enrichment in metastatic disease. A more immunosuppressive tumor microenvironment (TME) in $KRAS^{G12D}$ lung cancer tumors has been reported[28,31]. In a $KRAS^{G12D}$ mutation driven PDAC mice model, immune suppressive cytokines IL-4 and IL-13 and remodeling of the myeloid cell composition in TME have been demonstrated[40,41]. In PDAC mouse models treated with the $KRAS^{G12D}$ inhibitor MRTX 1133, increased macrophages (CD11b and F4/80+)

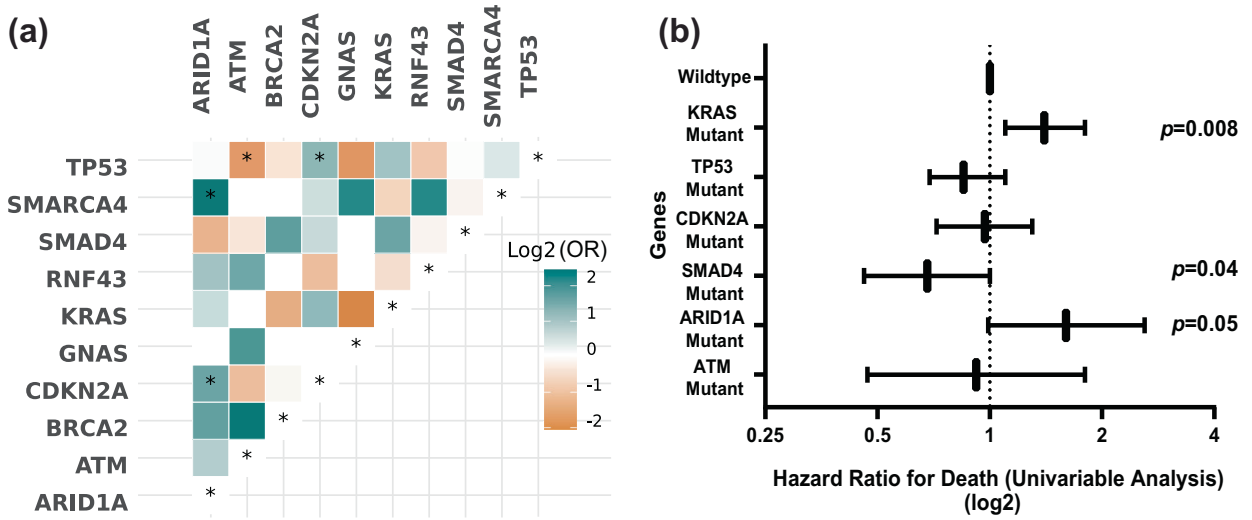

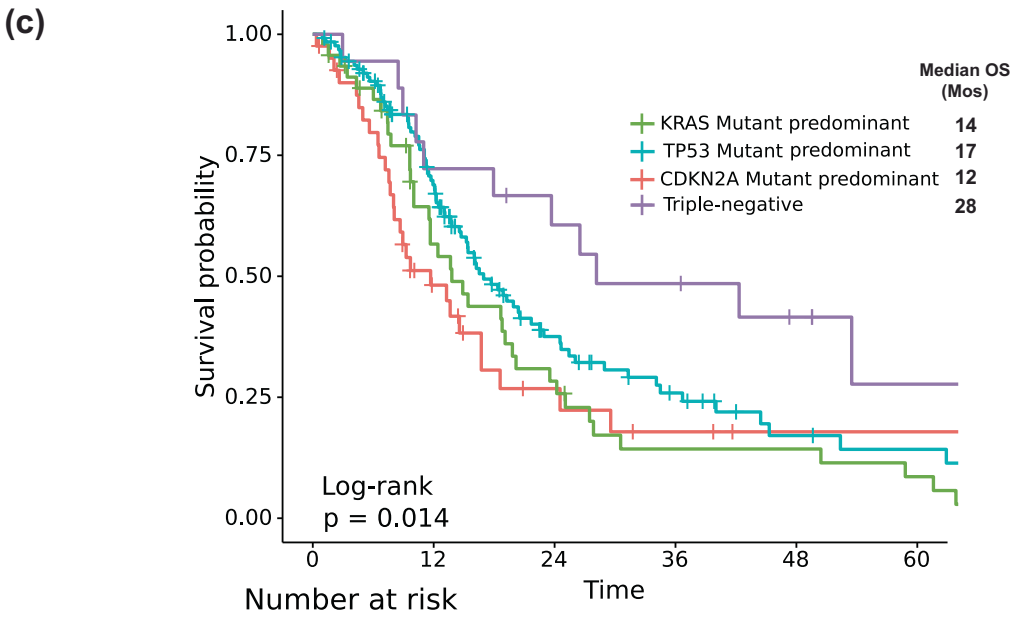

	KRAS	TP53	CDKN2A						
***KRAS* Predominant**	Mut	WT	WT	46	22	11	5	5	3
***TP53* Predominant**	± Mut	Mut	WT	127	75	28	15	7	5
***CDKN2A* Predominant**	± Mut	± Mut	Mut	41	15	6	3	1	1
Triple negative	WT	WT	WT	18	13	10	8	5	2

Fig. 5 Co-mutation with KRAS and OS analysis of MDA cohort. a Co-mutation analysis of the MD Anderson cohort. Associations between prevalent driver mutations were assessed using Fisher's exact method and a significant FDR-corrected p indicated by asterixis (*FDR-corrected $p < 0.1$). **b** Forest plot showing HR for death (from a univariable analysis) for driver mutations in our cohort, wildtype of each gene was used as reference. **c** KM OS analysis in patients with metastatic PDAC stratified by molecular subtype.

Table 2. PanCan validation cohort patient characteristics.

All	408 (100%)
Age, years–median (range)	65 (36,88)
Race/ethnicity	
Asian	8 (2.0%)
Black or African	12 (2.9%)
Hispanic or Latino	4 (1.0%)
White or Caucasian	174 (42.6%)
Other	1 (0.2%)
Not available	213 (52.2%)
Sex	
Female	188 (46.1%)
Male	220 (53.9%)
Histology grade	
Well-differentiated	6 (1.5%)
Moderately differentiated	78 (19.1%)
Poorly differentiated	46 (11.3%)
Not available	278 (68.1%)
Stage at diagnosis	
I	17 (4.2%)
II	16 (3.9%)
III	34 (8.3%)
IV	97 (23.8%)
Not available	244 (59.8%)
KRAS ($n = 408$)	
Mutant	377 (92.4%)
Wildtype	31 (7.6%)
TP53 ($n = 408$)	
Mutant	316 (77.5%)
Wildtype	92 (22.5%)
CDKN2A ($n = 408$)	
Mutant	86 (21.1%)
Wildtype	322 (78.9%)
SMAD4 ($n = 408$)	
Mutant	97 (23.7%)
Wildtype	311 (76.2%)
OS, months—median (range)	22 (0.2, 93)

Wildtype: denotes no pathogenic mutations were detected.

in the TME and decreased total myeloid cells was observed[42]. Correlative tissue and blood samples for potential *KRAS* mutation allele-specific immune features were not included in this project and could be a future research direction in patients with PDAC.

KRAS^{G12R} was more common in PDAC (~15%) than in other cancer types[12]. It has distinct biochemical features from *KRAS*$^{G12D/V}$ including an altered switch-II structure that cannot activate p110α/PI3K directly[43]. We found the median OS of patients with a *KRAS*^{G12R} mutation was comparable to that in patients with wildtype *KRAS* and longer than that in patients with *KRAS*^{G12D} or *KRAS*^{Q61} mutations. There was enrichment of *KRAS*^{G12R} mutation in well and moderately differentiated tumors vs poorly differentiated/anaplastic tumors (OR: 1.7, 95% CI 1.05–2.99, $p = 0.04$) (Fig. 3d), which suggested less aggressive biology and better outcome for the *KRAS*^{G12R}-mutated tumors. On the other hand, *KRAS*^{Q61} mutant tumors had a decreased GTP hydrolysis rate with high RAF-dependent MEK phosphorylation, and they did not response to SOS1 inhibition[29,44]. While *KRAS*^{Q61} mutants had shorter median OS in our cohort, little is known about the clinical features of this *KRAS* mutation subtype. To our knowledge, this is the first study to report worse OS with *KRAS*^{Q61}, which could be consistent with its biochemical features. Due to the rarity of *KRAS*^{Q61} mutations, we grouped different *KRAS*^{Q61} mutations together, though the association with OS may be mutant-specific[45]. The clinical and molecular features of *KRAS*^{G12R}- and *KRAS*^{Q61}-mutated PDAC warrant further investigation; additional research in larger populations could help the development of *KRAS* allele-specific inhibitors such as the *KRAS*^{G12R} inhibitor[46].

Co-mutations with *KRAS* could be one of the contributing factors for the allele specific clinical outcomes in PDAC. *KEAP1* co-mutation with *KRAS* in lung cancer was associated with early progression on the *KRAS*^{G12C} inhibitor sotorasib[25]. Co-occurrence of other mutations were common in PDAC, and the disease progression model proposed based on observed co-mutation patterns was early *KRAS* mutation followed by *CDKN2A* then loss of *TP53* and *SMAD4*[47,48]. Our data were consistent with previous reports that *TP53* (67%) was the most common co-mutation with *KRAS* followed by *CDKN2A* (17%), *SMAD4* (11%), and *ARID1A* (6%) (Fig. 4b)[12]. We tested the *KRAS/CDKN2A/TP53* disease progression model by classified four distinct molecular subtypes of metastatic patients in patients who had been tested for *KRAS*, *TP53*, and *CDKN2A* mutations ($n = 232$). We found patients with triple negative (*KRAS−/TP53−/CDKN2A−)* tumors demonstrated the best OS (median 28 months) while *CDKN2A* predominant tumors had the worst OS (median OS12 months, $p = 0.014$) (Fig. 5c). In our study, *CDKN2A* mutation included any mutation (either missense or deletion of *CDKN2A)*. Germline *CDKN2A* mutation is associated with an increased risk of melanoma and pancreatic cancer, and somatic *CDKN2A* loss is common in pancreatic cancer[49–51]. Patients with resected PDAC and somatic *CDKN2A* loss had worse survival (median DFS 11.5 and OS 19.7) compared to patients with wildtype *CDKN2A* (median DFS 14.8 and median OS 24.6)[39]. In another study of 100 patients with PDAC (both metastatic and nonmetastatic included), *CDKN2A* mutations were also associated with shorter OS (22 months vs 35 months; $P = 0.018$)[52]. In *KRAS*-mutated lung cancer, *CDKN2A* mutation was associated with worse survival on imunotherapy[53]. In a mouse model, *CDKN2A* loss accelerated *KRAS*^{G12D}-driven tumor growth[54]. A therapeutic approach targeting *CDKN2A* in *KRAS*-mutated PDAC is under investigation; however, clinical activity of CDK4/6 inhibitors was not seen in early-phase trials[55,56]. The location of the methylthioadenosine phosphorylase gene (*MTAP*) is adjacent to *CDKN2A* and the majority of PDAC tumors with *CDKN2A* loss also had *MTAP* loss[57–59]. The surrogate role of *CDKN2A* is not clear, and the reported rate of *MTAP* loss in our cohort was low; the detection method for *MTAP* loss has not yet validated by comparative genomic hybridization for pancreatic cancer in our NGS testing panel.

Univariate OS analysis in our study did not show statistically significant association of either *TP53* or *CDKN2A* co-mutation with OS, but we did find that *ARID1A* mutation was associated with poor OS (median 18 vs 31 months, HR: 1.6, 95% CI 0.99–2.6, $p = 0.05$), and *SMAD4* mutation was associated with better OS (median 35 vs 27 months, HR: 0.67, 95% CI 0.46–0.99, $p = 0.046$) (Fig. 5b). *SMAD4* is a tumor suppressor gene, and reported results about the prognostic value of *SMAD4* have been inconsistent[39,60–62]. While an association between *SMAD4* inactivation in resected PDAC and poor prognosis has been reported, a separately reported meta-analysis did not show association between *SMAD4* mutation and OS[61,62]. Our data showed a 13% *SMAD4* mutation rate, and it was associated with better OS. Further studies with larger sample sizes and different populations are needed to reconcile these varying results. *ARID1A* was found to be significantly co-mutated with *CDKN2A* (OR: 2.7, 95% CI 1.18–6.02, FDR-corrected $p = 0.095$), and with *SMARCA4* (OR: 5.17, 95% CI 1.15–18.44, FDR-corrected $p = 0.1$). *KRAS*^{G12R} mutated

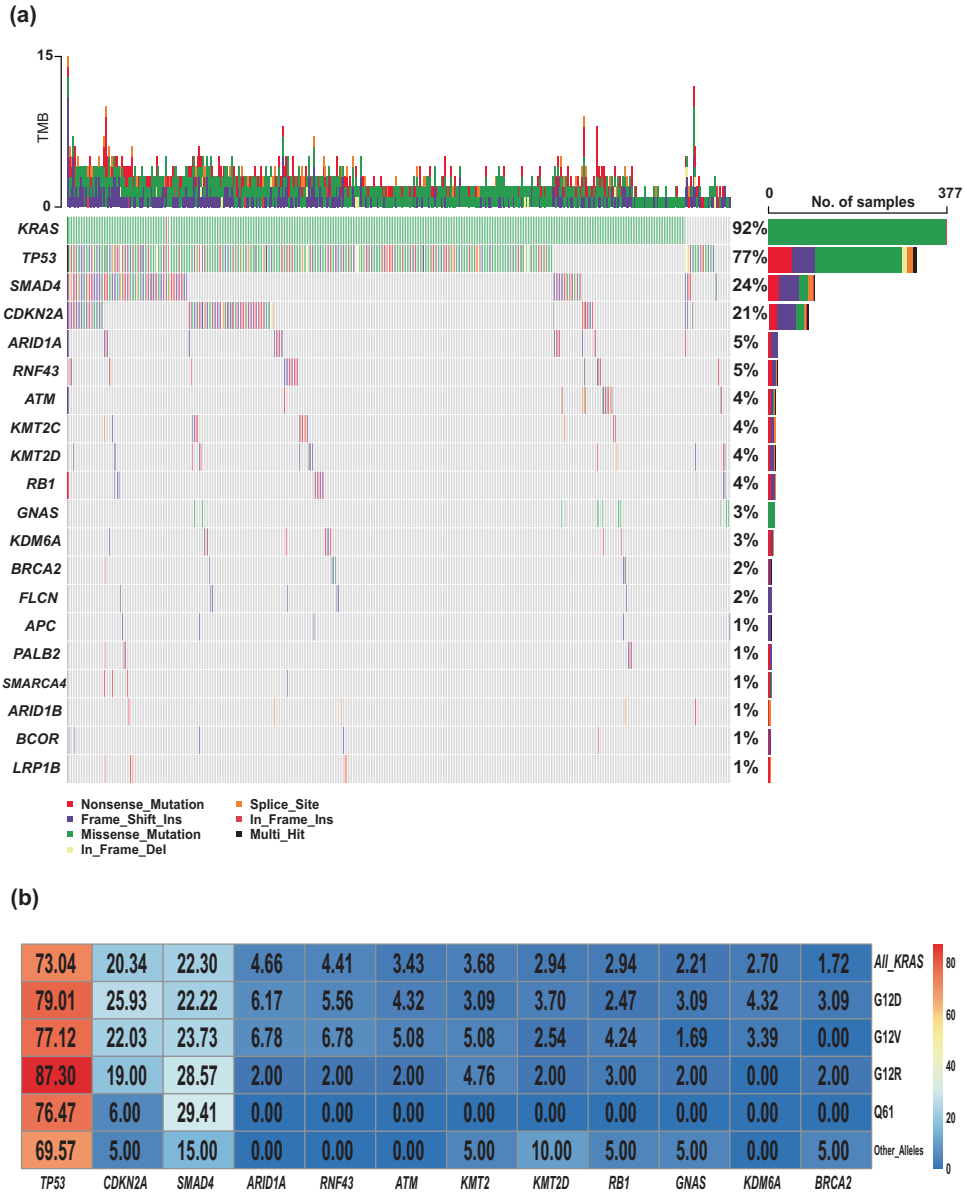

Fig. 6 Allele-specific co-mutations with KRAS of KYT cohort. a Oncoplot showing the somatic mutation distribution across the KYT cohort. **b** Heatmap showing the co-mutation landscape of the different *KRAS* mutation subtypes with the different genes and their frequencies in KYT cohort.

patients had lower rates of *ARID1A* co-mutation compared with $KRAS^{G12D}$ (0% vs 8% in $p = 0.02$) (Fig. 4b). Similar findings were also observed in the validation cohort from the PanCAN KYT® dataset. Both *ARID1A* and *SMARCA4* are Switch/Sucrose Non-fermentable (SWI/SNF) chromatin remodeling complex genes that are important for epigenetic reprogramming in PDAC[63]. Context-specific tumor suppressive or oncogenic functions of SWI/SNF chromatin regulation was noticed in PDAC[64,65]. In mouse models, disrupted *ARID1A* promoted the carcinogenesis from *KRAS*-mutated premalignant intraductal papillary mucinous neoplasms (IPMN) to PDAC[44]. In *KRAS*-mutated colon cancer, a similar tumor-supporting role of *ARID1A* was required for MEK/ERK signaling[66]. Our results of worse OS with *ARID1A* mutation support the oncogenic role of *ARID1A* and the potential benefit of targeting *ARID1A* in PDAC. *ARID1A* regulates DNA damage checkpoints and sensitizes cells to DNA damage response (DDR) targeting agents[67–69]. The ATM-TP53 signaling pathway is critical in DDR targeting in pancreatic cancer[70]. Interestingly, in both of our cohorts, *TP53* mutation was mutually exclusive with *ATM* mutation. Our findings of worse OS with *ARID1A* mutation and mutual exclusivity of *TP53* and *ATM* mutation in PDAC provided insights on PDAC therapeutic vulnerabilities.

The limitations of this study are heterogeneities in both patient populations and tumor mutation testing methods and gene panels. Only patients who had tissue molecular testing done at MD Anderson were included in this study; patients who had tests performed on other panels were not included. This is a retrospective study in a single tertiary cancer institution with ascertainment bias. The external validation cohort had limited clinical information, and treatment history was not available. Tumor genomic factors may not be the main contributor for *KRAS* mutation allele specificities. Correlative tissue and blood samples from patients were not available to evaluate other non-genomic factors that may account for the differences in clinical outcome observed.

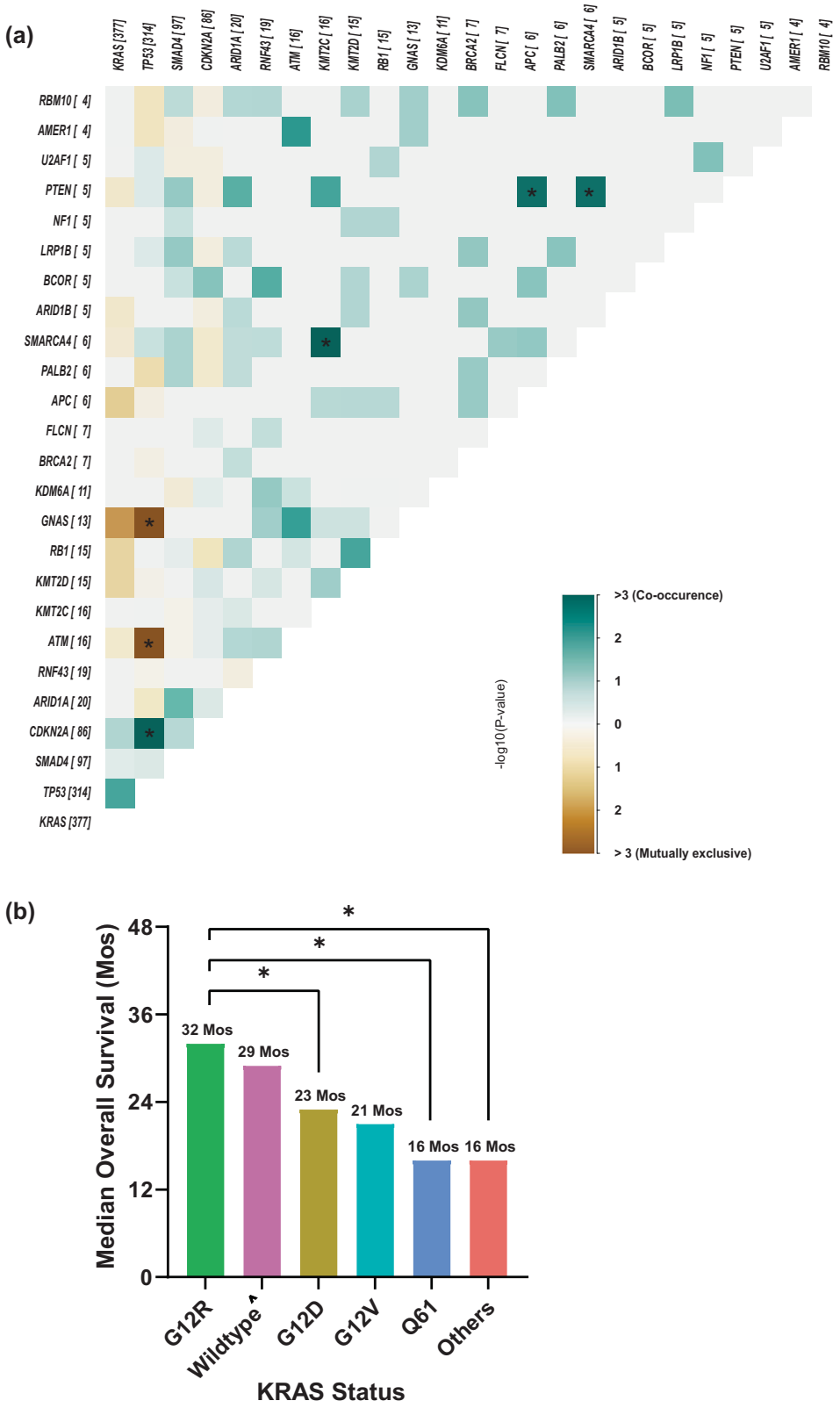

Fig. 7 Co-mutation analysis of KYT Cohort with OS. a Co-mutation analysis of KYT cohort, associations between prevalent driver mutations were assessed using the Fisher's exact method and a significant FDR-corrected p indicated by asterixis (*FDR-corrected $p < 0.1$). **b** Bar plot showing the difference in median overall survival between different *KRAS* mutation subtypes. * indicate $p < 0.05$ using log-rank test for survival. ^Wildtype: indicate no pathogenic mutations were detected.

In summary, we reported the *KRAS* mutation allele-specific clinical outcomes in patients with PDAC using a single institution retrospective study and an external validation cohort. Our findings suggested that *KRAS* targeting and combination strategies may warrant mutant allele-specific approaches with consideration of the mutations co-occurring with *KRAS*. In our analysis of 803 patients with PDAC, we found that *KRAS* mutation status and mutation allele subtypes were associated with OS. Patients with *KRAS* wildtype and $KRAS^{G12R}$-mutated tumors survived longer than patients with $KRAS^{G12D}$ or $KRAS^{Q61}$-mutated tumors, and this observation was confirmed in an external validation cohort. We also found enrichment of $KRAS^{G12D}$ mutations in patients with metastatic disease and $KRAS^{G12R}$ mutations in patients with well to moderately differentiated tumors. Moreover, we found co-mutations could contribute to *KRAS* allele-specific clinical outcomes. We found worse OS in *ARID1A*-mutated patients and a lower co-mutation rate of *ARID1A* in $KRAS^{G12R}$. Our findings of different clinical outcomes by *KRAS* mutation subtypes and co-mutation status suggest an allele- and co-mutation-specific impact of *KRAS* mutations on pancreatic cancer outcomes and provide guidance in improving approaches to target *KRAS* in pancreatic cancer.

METHODS

The MD Anderson Cancer Center Institutional Review Board (IRB) approved the collection of demographic, clinical, and pathological information under IRB protocols 09-0373 and 2023-0091. This study using human data complied with all relevant ethical regulations including the Declaration of Helsinki. Informed consent was waived, as per the IRB guidelines for retrospective studies of previously collected clinical and molecular information. The Palantir Foundry software system (Palantir, Denver, CO) was used to query the MD Anderson EHR to identify patients with a confirmed diagnosis of PDAC who underwent somatic tumor tissue mutation testing at MD Anderson from 3/14/1997 to 4/27/2023 for inclusion in the study.

Patient demographic, histopathology, tumor grade, surgical history, and mutational profile data were collected from the MD Anderson EHR and tumor registry data using the Foundry system. Histologic classification and grade were collected from the patients' pathology reports. Molecular testing was performed at MD Anderson's molecular diagnostics laboratory, which is College of American Pathologists (CAP) accredited and Clinical Laboratory Improvement Amendments (CLIA) certified. The gene panels used evolved during the study inclusion period, with expanding lists of genes over time. The information on tumor genomic alterations (GAs) was extracted from the available clinical and molecular data. Deidentified information was used for analysis.

For the co-mutation analysis, only patients who were tested with multigene panels were included ($n = 513$). The Oncoplot function within MAFtools was used to visualize the somatic mutation distribution. The function performs pair-wise Fisher's exact test to uncover mutually exclusive or co-occurring gene sets and an FDR-corrected $p < 0.1$ was considered significant. To better understand the co-mutation patterns with *KRAS* and the rest of the genes, a heatmap was constructed to demonstrate the co-mutation landscape of *KRAS* mutation status, as well as the status of the different *KRAS* alleles, and the rest of the genes analyzed (Fig. 4b). The percentage of co-occurrence between *KRAS* alleles and pathogenic mutations in the genes listed in the heatmap were determined using in-house R scripts. Fisher's exact test was used to test for significance in co-occurrence between *KRAS* alleles and pathogenic mutations. Based on the co-mutation patterns observed, we divided patients into 4 molecularly distinct PDAC co-mutation subtypes to visualize and test the relationship between co-mutation pattern and OS.

Statistical analysis

Differences in disease stage and tumor grade between patients with different *KRAS* mutations were assessed using Chi-square and Fischer's exact tests. Overall survival (OS) was calculated from the date of initial diagnosis until death or last known contact. OS curves were estimated using the Kaplan–Meier method, and the difference in survival curves was tested using the log-rank test. Univariate Cox proportional hazards models were used to estimate hazard ratios (HRs) and test the associations of *KRAS* mutation status, *KRAS* mutation allele subtypes, and other driver mutations with OS.

In the co-mutation analysis, the somatic interactions function within MAFtools was used to detect mutually exclusive or co-occurring mutation events. Pair-wise Fisher's exact test was used to uncover mutually exclusive or co-occurring gene sets with Benjamini–Hochberg multiplicity correction, and a false discovery rate (FDR)-corrected $p < 0.1$ was considered significant. The OS curves for the 4 co-mutation subtypes were estimated with the Kaplan–Meier method and compared using the log-rank test.

GraphPad Prism version 9 (GraphPad Software, San Diego, California USA) and Rstudio 2020 (RStudio, PBC. Boston, MA) were used for the statistical analyses and data visualization[71]. All tests were two-sided, and statistical significance was identified by a p-value < 0.05.

PanCAN's know your Tumor® program and dataset

PanCAN, in partnership with Tempus (Tempus Labs Inc., Chicago, IL), offers the Know Your Tumor® (KYT) precision medicine service to patients with pancreatic cancer. KYT data is available through the PanCAN SPARK platform (www.pancan.org/spark). Tempus processes, sequences and conducts group-level bioinformatics analyses on tumor biopsy samples. Data is derived from the Tempus xT NGS panel that covers 648 genes with actionable oncologic mutations. Variants are called from the resulting alignment files using an analysis pipeline that detects SNPs and indels using Freebayes and Pindel[72,73]. A filtered variant file that contains biologically relevant DNA variants, as determined by the Tempus pipeline, were used for all KYT-related analyses. Patients with PDAC who had their tumor sequenced by Tempus were included in the analysis. Pathogenic or likely pathogenic mutations were determined by Tempus' proprietary Knowledge Database which is based on the American College of Medical Genetics and Genomics (ACMG) and Association for Molecular Pathology (AMP) guidelines for variant classification. All mutation data was converted to Mutation Annotation Format (MAF) to enable use of the functions in the Bioconductor R package, MAFtools[74]. The Oncoplot function within MAFtools was used to visualize the somatic mutation distribution across the KYT cohort. The somatic interactions function within MAFtools was used to detect mutually exclusive or co-occurring mutation events. The function performs pair-wise Fisher's exact test to uncover mutually exclusive or co-occurring gene sets with Benjamini-Hochberg multiplicity correction, and an FDR-corrected $p < 0.1$ was considered significant. The percentage of co-occurrence between *KRAS* alleles and pathogenic mutations in the genes listed in the heatmap in Fig. 6 were determined using in-house R scripts. Fisher's exact test was used to test for significance in co-occurrence between *KRAS* alleles and other pathogenic mutations. Overall survival (OS) was calculated from the date of initial diagnosis until death or last known contact. OS curves by *KRAS* mutation and subtype status were estimated using the Kaplan–Meier method, and the difference in survival curves was tested using the log-rank test.

Reporting summary

Further information on research design is available in the Nature Research Reporting Summary linked to this article.

DATA AVAILABILITY

The data generated in this study are available upon request from the corresponding author. The MD Anderson institutional IRB does not allow for these data to be deposited into an external repository. PanCAN KYT data is available for access upon completion of a data-sharing agreement on the following domain: pancan.org/spark.

CODE AVAILABILITY

No custom code was used in this study. Details of bioinformatics analytics are available upon request.

Received: 22 July 2023; Accepted: 5 January 2024;
Published online: 03 February 2024

REFERENCES

1. Mizrahi, J. D., Surana, R., Valle, J. W. & Shroff, R. T. Pancreatic cancer. *Lancet* **395**, 2008–2020 (2020).
2. Rahib, L., Wehner, M. R., Matrisian, L. M. & Nead, K. T. Estimated projection of US cancer incidence and death to 2040. *JAMA Network Open* **4**, e214708–e214708 (2021).
3. Conroy, T. et al. FOLFIRINOX versus gemcitabine for metastatic pancreatic cancer. *N. Engl. J. Med.* **364**, 1817–1825 (2011).
4. Tempero, M. A. et al. Pancreatic adenocarcinoma, version 2.2021, NCCN clinical practice guidelines in oncology. *J. Natl. Compr. Canc. Netw.* **19**, 439–457 (2021).
5. Von Hoff, D. D. et al. Increased survival in pancreatic cancer with nab-paclitaxel plus gemcitabine. *N. Engl. J. Med.* **369**, 1691–1703 (2013).
6. Wang-Gillam, A. et al. Nanoliposomal irinotecan with fluorouracil and folinic acid in metastatic pancreatic cancer after previous gemcitabine-based therapy (NAPOLI-1): a global, randomised, open-label, phase 3 trial. *Lancet* **387**, 545–557 (2016).
7. Biankin, A. V. et al. Pancreatic cancer genomes reveal aberrations in axon guidance pathway genes. *Nature* **491**, 399–405 (2012).
8. Jones, S. et al. Core signaling pathways in human pancreatic cancers revealed by global genomic analyses. *science* **321**, 1801–1806 (2008).
9. Waters, A. M. & Der, C. J. KRAS: the critical driver and therapeutic target for pancreatic cancer. *Cold Spring Harb. Perspect. Med.* **8**, a031435 (2018).
10. Cancer Genome Atlas Research Network. Electronic address aadhe, Cancer Genome Atlas Research N. Integrated genomic characterization of pancreatic ductal adenocarcinoma. *Cancer Cell* **32**, 185–203.e113 (2017).
11. Bailey, P. et al. Genomic analyses identify molecular subtypes of pancreatic cancer. *Nature* **531**, 47–52 (2016).
12. Lee, J. K. et al. Comprehensive pan-cancer genomic landscape of KRAS altered cancers and real-world outcomes in solid tumors. *NPJ Precis. Oncol.* **6**, 91 (2022).
13. Ostrem, J. M., Peters, U., Sos, M. L., Wells, J. A. & Shokat, K. M. K-Ras(G12C) inhibitors allosterically control GTP affinity and effector interactions. *Nature* **503**, 548–551 (2013).
14. Canon, J. et al. The clinical KRAS(G12C) inhibitor AMG 510 drives anti-tumour immunity. *Nature* **575**, 217–223 (2019).
15. Govindan, R. et al. Phase 1 study of AMG 510, a novel molecule targeting KRAS G12C mutant solid. *Ann. Oncol.* **860**, v159–v193 (2019).
16. Hong, D. S. et al. KRAS(G12C) inhibition with sotorasib in advanced solid tumors. *N. Engl. J. Med.* **383**, 1207–1217 (2020).
17. Hallin, J. et al. The KRAS(G12C) inhibitor MRTX849 provides insight toward therapeutic susceptibility of KRAS-mutant cancers in mouse models and patients. *Cancer Discov.* **10**, 54–71 (2020).
18. Skoulidis, F. et al. Sotorasib for lung cancers with KRAS p.G12C mutation. *N. Engl. J. Med.* **384**, 2371–2381 (2021).
19. Strickler, J. H. et al. Sotorasib in KRAS p.G12C–mutated advanced pancreatic cancer. *N. Engl. J. Med.* **388**, 33–43 (2022).
20. Bekaii-Saab T. S. et al. Adagrasib in advanced solid tumors harboring a KRASG12C mutation. *J. Clin. Oncol.* **41**, 4097–4106.
21. Hallin, J. et al. Anti-tumor efficacy of a potent and selective non-covalent KRAS(G12D) inhibitor. *Nat. Med.* **28**, 2171–2182 (2022).
22. Tokatlian, T. et al. Chimeric antigen receptors directed at mutant KRAS exhibit an inverse relationship between functional potency and neoantigen selectivity. *Cancer Res. Commun.* **2**, 58–65 (2022).
23. Leidner, R. et al. Neoantigen T-cell receptor gene therapy in pancreatic cancer. *N. Engl. J. Med.* **386**, 2112–2119 (2022).
24. Jänne, P. A. et al. Adagrasib in non–small-cell lung cancer harboring a KRASG12C mutation. *N. Engl. J. Med.* **387**, 120–131 (2022).
25. Dy, G. K. et al. Long-term outcomes and molecular correlates of sotorasib efficacy in patients with pretreated KRAS G12C-mutated non–small-cell lung cancer: 2-year analysis of CodeBreaK 100. *J. Clin. Oncol.* **41**, 3311–3317 (2023).
26. Johnson, C., Burkhart, D. L. & Haigis, K. M. Classification of KRAS-activating mutations and the implications for therapeutic intervention. *Cancer Discov.* **12**, 913–923 (2022).
27. Hobbs, G. A. & Der, C. J. RAS mutations are not created equal. *Cancer Discov.* **9**, 696–698 (2019).
28. Ricciuti, B. et al. Comparative analysis and isoform-specific therapeutic vulnerabilities of KRAS mutations in non-small cell lung cancer. *Clinical Cancer Res.* **28**, 1640–1650 (2022).
29. Hunter, J. C. et al. Biochemical and structural analysis of common cancer-associated KRAS mutations. *Mol. Cancer Res.* **13**, 1325–1335 (2015).
30. Kobayashi, Y. et al. Silent mutations reveal therapeutic vulnerability in RAS Q61 cancers. *Nature* **603**, 335–342 (2022).
31. Ricciuti, B. et al. Dissecting the clinicopathologic, genomic, and immunophenotypic correlates of KRAS(G12D)-mutated non-small-cell lung cancer. *Ann. Oncol.* **33**, 1029–1040 (2022).
32. Rachakonda, P. S. et al. Somatic mutations in exocrine pancreatic tumors: association with patient survival. *PLoS One* **8**, e60870 (2013).
33. Skoulidis, F. & Heymach, J. V. Co-occurring genomic alterations in non-small-cell lung cancer biology and therapy. *Nat. Rev. Cancer* **19**, 495–509 (2019).
34. Diehl, A. C. et al. KRAS mutation variants and co-occurring PI3K pathway alterations impact survival for patients with pancreatic ductal adenocarcinomas. *Oncologist* **27**, 1025–1033 (2022).
35. Alfaro-Munoz, K. et al. Building a data foundation: how MD anderson and palantir are partnering to accelerate research and improve patient care. *J. Clin. Oncol.* **37**, e18077–e18077 (2019).
36. Zeineddine, F. A. et al. Survival improvement for patients with metastatic colorectal cancer over twenty years. *NPJ Precis. Oncol.* **7**, 16 (2023).
37. Goldstein, J. B. et al. Tackling "big data" for accelerating cancer research. *J. Clin. Oncol.* **34**, e23160–e23160 (2016).
38. Pishvaian, M. J. et al. Molecular profiling of patients with pancreatic cancer: initial results from the know your tumor initiative. *Clin. Cancer Res.* **24**, 5018–5027 (2018).
39. Qian et al. Association of alterations in main driver genes with outcomes of patients with resected pancreatic ductal adenocarcinoma. *JAMA Oncol.* **4**, e173420–e173420 (2018).
40. Hou, P. et al. Tumor microenvironment remodeling enables bypass of oncogenic KRAS dependency in pancreatic cancer. *Cancer Discov.* **10**, 1058–1077 (2020).
41. Dey, P. et al. Oncogenic KRAS-driven metabolic reprogramming in pancreatic cancer cells utilizes cytokines from the tumor microenvironment. *Cancer Discov.* **10**, 608–625 (2020).
42. Kemp, S. B. et al. Efficacy of a small-molecule inhibitor of KrasG12D in immunocompetent models of pancreatic cancer. *Cancer Discov.* **13**, 298–311 (2023).
43. Hobbs, G. A. et al. Atypical KRAS(G12R) mutant is impaired in PI3K signaling and macropinocytosis in pancreatic cancer. *Cancer Discov.* **10**, 104–123 (2020).
44. Kimura, Y. et al. ARID1A maintains differentiation of pancreatic ductal cells and inhibits development of pancreatic ductal adenocarcinoma in mice. *Gastroenterology* **155**, 194–209.e192 (2018).
45. Huynh, M. V. et al. Functional and biological heterogeneity of KRAS(Q61) mutations. *Sci. Signal.* **15**, eabn2694 (2022).
46. Zhang, Z., Morstein, J., Ecker, A. K., Guiley, K. Z. & Shokat, K. M. Chemoselective covalent modification of K-Ras(G12R) with a small molecule electrophile. *J. Am. Chem. Soc.* **144**, 15916–15921 (2022).
47. Hu, H.-f et al. Mutations in key driver genes of pancreatic cancer: molecularly targeted therapies and other clinical implications. *Acta Pharmacologica Sinica* **42**, 1725–1741 (2021).
48. Notta, F. et al. A renewed model of pancreatic cancer evolution based on genomic rearrangement patterns. *Nature* **538**, 378–382 (2016).
49. Vasen, H. F. et al. Risk of developing pancreatic cancer in families with familial atypical multiple mole melanoma associated with a specific 19 deletion of p16 (p16-Leiden). *Int. J. Cancer* **87**, 809–811 (2000).
50. Maitra, A. & Hruban, R. H. Pancreatic cancer. *Annu. Rev. Pathol.* **3**, 157–188 (2008).
51. Klatte, D. C. F. et al. Pancreatic cancer surveillance in carriers of a germline CDKN2A pathogenic variant: yield and outcomes of a 20-year prospective follow-up. *J. Clin. Oncol.* **40**, 3267–3277 (2022).
52. Doyle, A. et al. The impact of CDKN2A mutations on overall survival in pancreatic adenocarcinoma. *J. Clin. Oncol.* **37**, 278–278 (2019).
53. Zhao, D. et al. Clinical and molecular features of KRAS-mutated lung cancer patients treated with immune checkpoint inhibitors. *Cancers* **14**, 4933 (2022).
54. Aguirre, A. J. et al. Activated Kras and Ink4a/Arf deficiency cooperate to produce metastatic pancreatic ductal adenocarcinoma. *Genes Dev.* **17**, 3112–3126 (2003).

55. Goodwin, C. M. et al. Combination therapies with CDK4/6 inhibitors to treat KRAS-mutant pancreatic cancer. *Cancer Res.* **83**, 141–157 (2023).
56. Baghdadi, T. A. et al. Palbociclib in patients with pancreatic and biliary cancer with CDKN2A alterations: results from the targeted agent and profiling utilization registry study. *JCO Precis. Oncol.* **3**, 1–8 (2019).
57. Hustinx, S. R. et al. Concordant loss of MTAP and p16/CDKN2A expression in pancreatic intraepithelial neoplasia: evidence of homozygous deletion in a noninvasive precursor lesion. *Mod. Pathol.* **18**, 959–963 (2005).
58. Ngoi, N. et al. Genomic classification of clinically advanced pancreatic ductal adenocarcinoma (PDAC) based on methylthioadenosine phosphorylase (MTAP) genomic loss (MTAP loss). *J. Clin. Oncol.* **40**, 604–604 (2022).
59. Hustinx, S. R. et al. Homozygous deletion of the MTAP gene in invasive adenocarcinoma of the pancreas and in periampullary cancer: a potential new target for therapy. *Cancer Biol. Ther.* **4**, 83–86 (2005).
60. Hahn, S. A. et al. DPC4, a candidate tumor suppressor gene at human chromosome 18q21.1. *Science* **271**, 350–353 (1996).
61. Shugang, X. et al. Prognostic value of SMAD4 in pancreatic cancer: a meta-analysis. *Transl. Oncol.* **9**, 1–7 (2016).
62. Su, H. & Wang, C. Prognostic value of SMAD4 in resectable pancreatic cancer. *Postępy Higieny i Medycyny Doświadczalnej* **76**, 324–332 (2022).
63. Shain, A. H. et al. Convergent structural alterations define SWItch/Sucrose Non-Fermentable (SWI/SNF) chromatin remodeler as a central tumor suppressive complex in pancreatic cancer. *Proc. Natl. Acad. Sci. USA* **109**, E252–E259 (2012).
64. Halbrook, C. J., Lyssiotis, C. A., Pasca di Magliano, M. & Maitra, A. Pancreatic cancer: advances and challenges. *Cell* **186**, 1729–1754 (2023).
65. Ferri-Borgogno, S. et al. Paradoxical role of AT-rich interactive domain 1A in restraining pancreatic carcinogenesis. *Cancers* **12**, 2695 (2020).
66. Sen, M. et al. ARID1A facilitates KRAS signaling-regulated enhancer activity in an AP1-dependent manner in colorectal cancer cells. *Clin. Epigenetics* **11**, 92 (2019).
67. Mandal, J., Mandal, P., Wang, T.-L. & Shih, I.-M. Treating ARID1A mutated cancers by harnessing synthetic lethality and DNA damage response. *J. Biomed. Sci.* **29**, 71 (2022).
68. Shen, J. et al. ARID1A deficiency impairs the DNA damage checkpoint and sensitizes cells to PARP inhibitors. *Cancer Discov.* **5**, 752–767 (2015).
69. Mullen, J., Kato, S., Sicklick, J. K. & Kurzrock, R. Targeting ARID1A mutations in cancer. *Cancer Treat. Rev.* **100**, 102287 (2021).
70. Crowley, F., Park, W. & O'Reilly, E. M. Targeting DNA damage repair pathways in pancreas cancer. *Cancer Metastasis Rev.* **40**, 891–908 (2021).
71. RStudio: integrated development for R RStudio, PBC; 2020. http://www.rstudio.com/.
72. Garrison EM, G. Haplotype-based variant detection from short-read sequencing. https://arxiv.org/pdf/1207.3907.pdf (2012).
73. Ye, K., Schulz, M. H., Long, Q., Apweiler, R. & Ning, Z. Pindel: a pattern growth approach to detect break points of large deletions and medium sized insertions from paired-end short reads. *Bioinformatics* **25**, 2865–2871 (2009).
74. Mayakonda, A., Lin, D. C., Assenov, Y., Plass, C. & Koeffler, H. P. Maftools: efficient and comprehensive analysis of somatic variants in cancer. *Genome Res.* **28**, 1747–1756 (2018).

ACKNOWLEDGEMENTS

This work was supported by the Col. Daniel Connelly Memorial Fund, the National Cancer Institute (Cancer Center Support Grant P30 CA016672), the Cancer Prevention & Research Institute of Texas (CPRIT, RR180035 to J.P.S.), and a Conquer Cancer Career Development Award (to J.P.S.). The Pancreatic Cancer Action Network (PanCAN) provided access to the validation dataset from PanCAN's Know Your Tumor® program. Any opinions, findings, and conclusions expressed in this material are those of the author(s) and do not necessarily reflect those of the American Society of Clinical Oncology® or Conquer Cancer.

AUTHOR CONTRIBUTIONS

D.Z. and J.P.S. conceptualized the paper, provided oversight, and contributed to patient enrollment and treatment, patient assessment, data interpretation, and writing the manuscript. D.Z., A.Y., and M.Y. conceived and designed the study and contributed to literature search, data acquisition, data analysis, data interpretation, and manuscript writing. J.W., M.O., and S.K. contributed to patient enrollment, treatment, assessment, and data interpretation. K.A., S.D., and L.M. contributed to data acquisition, data analysis, and data interpretation. M.K., P.E., S.C., J.P., and R.S. contributed to the statistical analysis and writing of the manuscript. All authors read, reviewed, and approved the final version of the manuscript.

COMPETING INTERESTS

D.Z. has clinical trial contracts with Mirati and CARsgen and served as a member of the advisory board for Affini-T.K.A., S.D., and L.M. are employees of the Pancreatic Cancer Action Network, a nonprofit cancer advocacy organization that receives donations from private and commercial entities and may benefit indirectly financially and non-financially from this publication. S.P. reports research funding from Mirati Therapeutics, Lilly, Xencor, Novartis, Rgenix, Bristol-Myers Squibb, Astellas Pharma, Framewave, 4D Pharma, Boehringer Ingelheim, NGM Biopharmaceuticals, Janssen, Arcus Biosciences, Elicio Therapeutics, Bionote, Ipsen, Zymeworks, Pfizer, Immuno-MET, Immuneering, Amal Therapeutics. S.P. is a member of the advisory board for Zymeworks, Ipsen, Novartis, Janssen, Boehringer Ingelheim, AskGene Pharma, BPGbio, Jazz Pharmaceuticals, AstraZeneca, US WorldMeds, Nihon Medi-Physics Co., Ltd., Alligator Bioscience. M.L. consults for Pfizer, Delcath, Janssen, BioNTech, G1 Therapeutics, Imvax, and Bayer and received research funding from institutions from EpimAb BioTherapeutics, Merck, Erasca, Boehringer Ingelheim, Arcus Biosciences, Repare Therapeutics, Trisalus Life Sciences, and Xilis. A.M. is a consultant for Tezcat Biotechnologies and is a co-inventor on a patent that has been licensed from Johns Hopkins University by Thrive Earlier Detection (an Exact Sciences company). A.M. serves on the scientific and medical advisory board for Pancreatic Cancer Action Network and Pancreatic Cancer UK. J.P.S. receives grants, research support, or collaborates with Celsius Therapeutics, BostonGene, Caris Life Sciences, Natera, Xilis, Palantir, and Genentech. J.P.S. reports consulting and stock ownership with Engine Biosciences, NaDeNo Nanoscience.

ADDITIONAL INFORMATION

Supplementary information The online version contains supplementary material available at https://doi.org/10.1038/s41698-024-00505-0.

Correspondence and requests for materials should be addressed to Dan Zhao.

Reprints and permission information is available at http://www.nature.com/reprints

Publisher's note Springer Nature remains neutral with regard to jurisdictional claims in published maps and institutional affiliations.